A MIXED FINITE ELEMENT METHOD FOR NONLINEAR DIFFUSION EQUATIONS

MARTIN BURGER, JOSÉ A. CARRILLO, MARIE-THERESE WOLFRAM

Abstract. We propose a mixed finite element method for a class of nonlinear diffusion equations, which is based on their interpretation as gradient flows in optimal transportation metrics. We introduce an appropriate linearization of the optimal transport problem, which leads to a mixed symmetric formulation. This formulation preserves the maximum principle in case of the semi-discrete scheme as well as the fully discrete scheme for a certain class of problems. In addition solutions of the mixed formulation maintain exponential convergence in the relative entropy towards the steady state in case of a nonlinear Fokker-Planck equation with uniformly convex potential. We demonstrate the behavior of the proposed scheme with 2D simulations of the porous medium equations and blow-up questions in the Patlak-Keller-Segel model.

1. Introduction

In this paper we consider the numerical solution of the nonlinear (and eventually nonlocal) diffusion equation

$$\frac{\partial \rho}{\partial t} = \operatorname{div}\left(\rho \nabla \left(U'\left(\rho\right) + V + W * \rho\right)\right) \qquad t > 0,\ x \in \mathbb{R}^d, \tag{1}$$

with $\rho(x,0) = \rho_0(x)$. Here ρ is a time-dependent density, $U\colon \mathbb{R}^+ \to \mathbb{R}$ an internal energy, $V\colon \mathbb{R}^d \to \mathbb{R}$ is a given external potential, and $W\colon \mathbb{R}^d \to \mathbb{R}$ is an interaction potential. By a density, we mean an $L^1(\mathbb{R}^d)$ nonnegative function with a given mass M, i.e., ρ/M is a probability density.

Equation (1) includes many well known equations like the heat equation with $U(\rho) = \rho \log \rho - \rho$ and $V = W = 0$, the porous medium equation (PME) and fast diffusion equation (FDE) with

$$U(\rho) = \frac{1}{m-1}\rho^m, \tag{2}$$

where $m > 0$ and $V = W = 0$, or the linear Fokker Planck equation with

$$U(\rho) = \rho \log \rho - \rho, \tag{3}$$

a given potential V and $W = 0$. The Patlak-Keller-Segel (PKS) model, describing the movement of cells in a chemoattractant, can also be interpreted in

1991 *Mathematics Subject Classification.* Primary: 35K55, 65M60; Secondary: 35Q84.

Key words and phrases. Nonlinear diffusion problems, optimal transportation problem, mixed finite element method, porous medium equation, Patlak-Keller-Segel model.

the formalism of (5). The original PKS model, introduced by E.F. Keller and L.A. Segel in 1970 is given by

$$\frac{\partial \rho}{\partial t} = \operatorname{div}\left(\nabla \rho - \chi \rho \nabla v\right) \qquad t > 0, x \in \mathbb{R}^d, \tag{4a}$$

$$\frac{\partial v}{\partial t} = k\Delta v - \alpha v + \rho \qquad t > 0, x \in \mathbb{R}^d, \tag{4b}$$

where ρ describes the density of cells, v the concentration of the chemical substrate and χ the sensitivity of the cells to the chemoattractant. Since the chemical reaction happens on a much faster time scale than the movement of cells, the term $\frac{\partial v}{\partial t}$ can be neglected. If $\alpha = 0$ we obtain the reduced PKS model where (4b) is replaced by $-\Delta v = \rho$, see [25, 11, 10, 17] and the references therein for an updated state of the results. This equation can be solved using the fundamental solution of the Poisson equation in $\mathbb{R}^d$, hence the reduced PKS model in spatial dimension two corresponds to (1) with $U = \rho \log \rho - \rho$, $V = 0$ and $W = \frac{\chi}{2\pi} \log|x|$.

Further examples can be found in modelling granular flows [6, 7], mathematical biology (cf. [28, 36]), and more general aggregation phenomena (cf. [14, 15, 8]), where W is an attractive interaction like in PKS (cf. [39] for the derivation from a microscopic model with nonlocal attraction and local repulsion). Finally, also electro-diffusion models can be put into the form (1), where $W * \rho$ corresponds to the electric potential generated by the charge density. Due to the repulsive nature of electrical forces, W has opposite sign as in the PKS model or in aggregation. We finally mention that related numerical schemes have already been used for the simulation of transport through ion channels (cf. [16]).

All these equations have the same underlying structure - they can be interpreted as gradient flows with respect to the Wasserstein distance for the free energy or relative entropy functional E. Jordan, Kinderlehrer and Otto [34] showed that solutions of (1) in the linear Fokker-Planck case can be constructed using a variational scheme, known as JKO scheme. The gradient flow interpretation was first studied by Otto in the case of the PME [40] and later generalized to the family of equations of the form (1) in [21]. The variational scheme was shown to be convergent for this family of equations in [1] relating these schemes to the method of minimizing movements introduced by DeGiorgi [23]. We refer to [46, 1] for further information on the theory of optimal transportation problems and gradient flows.

A key ingredient of this gradient-flow interpretation of equations (1) is played by the Benamou-Brenier formula [5]. In fact, this formula provides an alternative and very useful way of writing the variational JKO schemes. For our purposes, we only state that the main consequence of all this new gradient-flow approach. Equation (1) can be interpreted as a limit of infinitesimal time increment in the optimality condition of the following variational problem related to optimal transport: Given a density ρ_{k-1} of mass M at time $t = t_{k-1}$, determine ρ_k at time $t = t_k$ of mass M, and an interpolating in time density ρ of mass M at each

time and a velocity field u such that

$$\inf_{(\rho,\rho_k,u)\in\mathcal{A}} \left\{ E(\rho_k) + \frac{1}{2}\int_{t_{k-1}}^{t_k}\int_{\mathbb{R}^d} \rho\,(x,t)\,|u\,(x,t)|^2\;dx\;dt \right\}, \tag{5a}$$

where $\mathcal{A}$ is the set of constraints given by the continuity equation with boundary values:

$$\begin{aligned} &\frac{\partial\rho}{\partial t} + \operatorname{div}(\rho u) = 0, \\ &\rho(\cdot,t_{k-1}) = \rho_{k-1}, \quad \rho(\cdot,t_k) = \rho_k. \end{aligned} \tag{5b}$$

Here the free-energy or entropy functional $E(\rho_k)$ is given by

$$\begin{aligned} E(\rho) = &\int_{\mathbb{R}^d} U(\rho(x))\,dx + \int_{\mathbb{R}^d} V(x)\rho(x)dx \\ &+ \frac{1}{2}\int_{\mathbb{R}^d\times\mathbb{R}^d} W(x-y)\rho(x)\rho(y)dxdy. \end{aligned} \tag{6}$$

This paper is concerned with the development of a numerical scheme that can be applied to a very general class of problems, given by (1). Various numerical methods for the PME or the PKS model have been introduced in literature, most capable of dealing with one or the other equation. These methods include for example a finite element approach of the one-dimensional PME by Jäger and Kačur [32], which has been extended to spatial dimension two by Mikula in [38]. Finite difference schemes to calculate the solution and/or the interface have been used in [43] or [24]. Westdickenberg and Wilkening presented a 1D variational particle scheme which is based on the optimal transport formulation of the PME, cf. [47].

The reduced PKS model in spatial dimension two exhibits an interesting feature, namely the finite time blow up of solutions under certain conditions on the initial data. Numerical schemes for the PKS model have been proposed by Marrocco [37] or Filbet in [27]. These methods have been used successfully to describe the behavior of solutions before the chemotactic collapse. Up to the authors knowledge the only methods capable of resolving blow up events have been developed by Blanchet, Calvez, and Carrillo in 1D [9], by Budd et. al. in [13], by Haškovec and Schmeiser in [29] and recently by Carrillo and Moll [18]. The last authors proposed a numerical scheme based on the Lagrangian formulation of the nonlinear Fokker-Planck equation, being actually a reformulation of the JKO scheme, see [18]. This approach has been used successfully for a very general class of partial differential equations, which include the PME as well as the PKS model. However, it increases the computational time. Our objective here is to propose a scheme in the Eulerian variables based on more standard finite element techniques for the optimization problem (5).

This paper is organized as follows: in Section 2 we present a special linearization of the optimal transportation formulation (5), the mixed finite element discretization, and discuss the mathematical analysis. The application of the linearized scheme to the PME and the FDE is presented in Section 3. We are able to verify a discrete maximum principle for the numerical scheme and present 2D numerical simulations. In Section 4 we apply the numerical scheme to the PKS model and illustrate the blow up behavior of solution with various numerical experiments. Finally, Section 5 presents an extension of the scheme to the case of external velocities and discusses stabilization techniques for this sake.

2. Discretization Approaches

In this Section we shall discuss our approach to the discretization of the nonlinear diffusion equation (1). We start with a time discretization arising from a linearization of the optimal transport formulation and then proceed to a spatial discretization by mixed finite elements, which seems rather natural for the arising optimality system.

2.1. Time-Stepping by Linearized Transport.

In the introduction we discussed the reformulation of the nonlinear diffusion problem (1) as an optimal transportation problem (5). Based on this optimal transport formulation we propose the following linearization: Given a density ρ_{k-1}, find ρ_k, ρ and u such that

$$\inf_{\rho,\rho_k,u} \left\{ E(\rho_k) + \frac{1}{2} \int_{t_{k-1}}^{t_k} \int_{\mathbb{R}^d} \rho_{k-1}(x) \, |u(x,t)|^2 \, dxdt \right\},$$

under the constraint that

$$\begin{aligned} &\frac{\partial \rho}{\partial t} + \operatorname{div}(\rho_{k-1} u) = 0, \\ &\rho(\cdot, t_{k-1}) = \rho_{k-1}, \quad \rho(\cdot, t_k) = \rho_k, \end{aligned}$$

is satisfied. This formulation corresponds to a quadratic expansion of the objective functional and a linearization of the constraint around the feasible point $\rho \equiv \rho_{k-1}$, $u \equiv 0$. The corresponding Lagrange functional $\mathcal{L}$ is given by

$$\begin{aligned} \mathcal{L} = E(\rho_k) + \int_{t_{k-1}}^{t_k} \int_{\mathbb{R}^d} \left[\frac{|u|^2}{2} \rho_{k-1} - \frac{\partial \mu}{\partial t} \rho - \rho_{k-1} (u \cdot \nabla \mu) \right] dxdt \\ - \int_{\mathbb{R}^d} \left[\mu(x, t_{k-1}) \rho_{k-1} - \mu(x, t_k) \rho_k \right] dx, \end{aligned}$$

where μ denotes the Lagrange parameter. Then the optimality conditions read as

$$u = \nabla \mu, \qquad \frac{\partial \mu}{\partial t} = 0 \quad \text{and} \quad \mu(t_k) = -\frac{\delta E}{\delta \rho}(\rho_k). \tag{7}$$

From (7) we deduce that μ is linear in time and obtain the following optimality condition

$$\frac{\rho_k - \rho_{k-1}}{\tau} = \operatorname{div}\left(\rho_{k-1}\nabla\left(U'\left(\rho_k\right) + V + W * \rho_k\right)\right), \tag{8}$$

with $\tau = t_k - t_{k-1}$. Note that equation (8) can be interpreted as a semi-implicit time-discretization of (1).

Finally, let us mention that the equation (1) can be studied in smooth bounded domains $\Omega \subset \mathbb{R}^d$ with no-flux boundary conditions. In order to do this, the functional (6) has to be restricted to densities supported in Ω and the continuity equation (5b) augmented with the boundary condition $u \cdot \eta = 0$ with η the outwards unit normal field to $\partial\Omega$. As a consequence, we can also consider the initial boundary value problem consisting of (1) with boundary condition

$$\nabla\left(U'\left(\rho\right) + V + W * \rho\right) \cdot \eta = 0 \tag{9}$$

on $\partial\Omega$ with $\Omega \in C^2$. For the rest of the paper we make the following assumptions.

(A1) Let $\Omega \subset \mathbb{R}^d$ be a smooth, bounded domain.
(A2) The external potential V is locally convex and satisfies $V \in W^{1,1}_{loc}(\Omega)$.
(A3) $U' \colon \mathbb{R}^+_0 \to \mathbb{R}$ is continuous, strictly increasing and $U(0) = 0$ with $U'(0+) = -\infty$ or $U'(\infty) = \infty$.

Existence and uniqueness of solutions for (8) can be shown under appropriate conditions on U and W, which however need to be examined in several different cases and are therefore omitted here. We are more interested in structural properties that are preserved by the linearization, and we restrict ourselves to the simplification $W \equiv 0$ for the sake of this investigation.

Let ρ_{s,M_1} and ρ_{s,M_2} denote stationary solutions of (8) with masses M_1 and M_2 satisfying

$$\rho_{k-1}\nabla\left(U'(\rho) + V(x)\right) = 0\,, \qquad \int_\Omega \rho \, dx = M_i \quad \text{for} \quad i = 1, 2. \tag{10}$$

If $\rho_{k-1}(x) > 0$ for all $x \in \Omega$, then the stationary solution ρ_s solves

$$U'(\rho) + V(x) = c \quad \text{for all} \quad x \in \Omega,$$

for some $c \in \mathbb{R}$. Hence $\rho_s = \sigma^{-1}(c - V(x))$, where σ denotes the generalized inverse of U', given by

$$\sigma^{-1} = \begin{cases} 0 & \text{if } c - V(x) \leq 0 \\ (U')^{-1} & \text{if } c - V(x) > 0. \end{cases}$$

The inverse function is well defined if $U'(0+) = -\infty$ and $U'(\infty) = \infty$. If $U'(0+) > -\infty$ or $U'(\infty) < \infty$, then the range of the function $c - V(x)$ may exceed the range interval $(U'(0+), U'(\infty))$. If assumption (A1)-(A3) hold, we can state the following existence and uniqueness result.

Lemma 2.1. [20] *Let (A1)-(A3) hold, then the stationary equation (10) together with the boundary conditions (9) admits a unique solution.*

Using the notion of stationary solutions we are able to verify the following maximum principle for the semi-implicit scheme (8).

Theorem 2.2. *Let assumptions* (A1)-(A3) *hold,* $W \equiv 0$*, and* $\rho_{k-1} \in L^\infty(\Omega)$ *with* $0 < \rho_{s,M_1}(x) \le \rho_{k-1}(x) \le \rho_{s,M_2}(x)$ *for all* $x \in \Omega$*. Here* ρ_{s,M_1} *and* ρ_{s,M_2} *denote the lower and upper stationary solution solving (10) together with (9). Then* $\rho(x)$*, solving the problem (8)-(9), satisfies*

$$\rho_{s,M_1}(x) \le \rho\,(x) \le \rho_{s,M_2}(x) \qquad \text{for all } x \in \Omega.$$

Proof. Since our main interest is on the fully discrete scheme to be analyzed later we will here only give a sketch of proof trying to avoid technicalities needed to obtain smooth approximations, but rather sketch the main lines, from which also some insight for the fully discrete case is gained. Note that for the stationary solutions, the potential $\mu = U'(\rho) + V$ is constant, hence the above maximum principle can be translated into a maximum principle for $\mu_k = U'(\rho_k) + V$, i.e. μ_k remains between the same constants as μ_{k-1}. We approximate (8) by

$$\frac{\rho_k - \rho^\epsilon_{k-1}}{\tau} + \epsilon\rho^\epsilon_{k-1} = \operatorname{div}\left(\rho^\epsilon_{k-1}\nabla\left(U'_\epsilon\left(\rho_k\right) + V^\epsilon\right)\right), \tag{11}$$

with $\epsilon > 0$, ρ^ϵ_{k-1} and V^ϵ being a smoothed version of ρ_{k-1} and V, and U^ϵ being a smooth approximation of U with $U'_\epsilon(0_+) = -\infty$. The equation is supplemented by homogeneous Neumann boundary conditions on $\partial\Omega$, i.e.

$$\left(\rho^\epsilon_{k-1}\nabla\left(U'_\epsilon\left(\rho_k\right) + V^\epsilon\right)\right)\cdot\eta = 0.$$

The approximate problem is a uniformly elliptic equation, thus $\rho_k \in C^2(\bar\Omega)$ can be obtained. Moreover due to standard convergence as $\epsilon \to 0$ it suffices to prove the maximum principle for this smoothed situation. For simplicity we also drop the index ϵ in the following.

Let us assume that there exists and $\bar x \in \bar\Omega$ such that μ_k attains a maximum in $\bar x$, hence also $U'(\rho(x)) - U'(\rho_{s,M_2}(x))$ attains its maximum at $\bar x$. Now let us assume that $U'(\rho(\bar x)) - U'(\rho_{s,M_2}(\bar x)) > 0$. Assumption (A3) implies that $\rho(\bar x) > \rho_{s,M_2}(\bar x)$. If $\bar x \in \Omega$, then from the standard properties of first and second derivatives for maxima and from (11), we conclude

$$0 < \epsilon\rho_{k-1} \le \rho_{k-1}\Delta\left(U'_\epsilon\left(\rho_k\right) + V^\epsilon\right)) = \rho_{k-1}\Delta\mu_k \le 0,$$

a contradiction. For $\bar x \in \partial\Omega$ we use the Neumann boundary condition (9) to conclude that indeed $\nabla\mu_k = 0$, since all tangential derivatives to $\partial\Omega$ vanish due to the maximum property. Hence, the Hessian matrix of ρ_k is negative semidefinite since otherwise a simple Taylor expansion will contradict the maximum property. If c is a lower bound on ρ_{k-1}, this can be used to show that

$$\frac{\epsilon c}{2} < \frac{\rho_k - \rho^\epsilon_{k-1}}{\tau} + \epsilon\rho^\epsilon_{k-1} = \operatorname{div}\left(\rho_{k-1}\nabla\left(U'_\epsilon\left(\rho_k\right) + V^\epsilon\right)\right) < \frac{\epsilon c}{2},$$

where the last inequality holds in a sufficiently small neighborhood of $\bar{x}$ inside Ω since $\rho_k \in C^2(\bar{\Omega})$, $\nabla \mu_k = 0$ and the Hessian matrix being negative semidefinite, a contradiction.

The same argument holds for the lower stationary solution ρ_{s,M_1} by replacing maximum by minimum and appropriate simple changes. □

Remark 1. In the PME/FD case, we can state the maximum principle in Theorem 2.2 in a much simpler manner: if $0 < c_1 \leq \rho_{k-1}(x) \leq c_2$ for all $x \in \Omega$ and $c_1, c_2 \in \mathbb{R}^+$, then the solution of the semi-implicit scheme (8) satisfies $0 < c_1 \leq \rho_{k-1}(x) \leq c_2$. This is due to a maximum principle that actually holds for the dual variable μ, Theorem 2.2 could be reformulated as follows (note that stationary solutions correspond to constant dual variables μ): If $0 < c_1 \leq \mu(0) \leq c_2$, then $0 < c_1 \leq \mu(t) \leq c_2$ for all $t > 0$. In this form we shall also investigate maximum principles for the discrete scheme.

Next we would like to study the long-time asymptotics of the semi-implicit scheme in (8). In recent years, the long time behavior of nonlinear diffusion equations and particularly the convergence of $\rho(t)$ towards equilibration as $t \to \infty$ has attracted lots of attention. These convergence estimates are usually stated in terms of the relative entropy (or relative free energy)

$$E(\rho|\rho_\infty) := E(\rho) - E(\rho_\infty), \tag{12}$$

where ρ_∞ denotes the stationary solution with the same mass M as $\rho(t)$ satisfying (10) and E is given by (6). The trend to equilibrium of the PME has been discussed in [22, 45], for the nonlinear Fokker-Planck equation see e.g. [2]. All results are based on functional inequalities and show exponential convergence towards the equilibrium in the relative entropy (12). The long time behavior of an implicit time-discrete linear Fokker-Planck equation has been studied by Arnold and Unterreiter (cf. [3]), and by Carrillo et al. in case of an implicit time-discrete nonlinear diffusion equation (cf. [19]). We are able to show that the proposed semi-implicit scheme preserves the long time behavior of the nonlinear diffusion equation with uniformly convex potentials V, i.e. the exponential decay of the relative energy functional (12).

Theorem 2.3. *Let all assumptions of Theorem 2.2 hold. Then ρ_k satisfies the following estimate*

$$E(\rho_k|\rho_\infty) \leq (1 + \lambda\kappa\tau)^{-k} E(\rho_0|\rho_\infty),$$

where λ is a positive constant and $\kappa \in \mathbb{R}^+$ depends on $\|\rho_{s,M_1}\|_{L^\infty}$ and $\|\rho_{s,M_2}\|_{L^\infty}$ only.

Proof. The relative entropy (12) can we written as

$$E(\rho|\rho_\infty) := \int_\Omega [U(\rho) - U(\rho_\infty) - U'(\rho_\infty)(\rho - \rho_\infty)]\, dx,$$

and the energy production $D(\rho) = -\frac{d}{dt}E(\rho)$ as

$$D(\rho) := \int_\Omega \rho|\nabla V + U''(\rho)\nabla\rho|^2 dx.$$

The generalized Log-Sobolev inequality [20] asserts that there exists an $\lambda > 0$ such that

$$E(\rho|\rho_\infty) \le \frac{1}{2\lambda} D(\rho), \tag{13}$$

using the uniform convexity of the potential V. Let ρ_k be the solution of (8), then we obtain

$$\begin{aligned}
E(\rho_k|\rho_\infty) &\ge \int_\Omega \left[U'(\rho_{k+1})\left(\rho_k - \rho_{k+1}\right) + U(\rho_{k+1}) - U(\rho_\infty) - U'(\rho_\infty)(\rho_k - \rho_\infty)\right] dx \\
&= \int_\Omega \left[U(\rho_{k+1}) - U(\rho_\infty) - U'(\rho_\infty)(\rho_{k+1} - \rho_\infty)\right] dx \\
&\quad + \int_\Omega \left[U'(\rho_\infty)(\rho_{k+1} - \rho_k) + U'(\rho_{k+1})\left(\rho_k - \rho_{k+1}\right)\right] dx \\
&= E(\rho_{k+1}|\rho_\infty) + \int_\Omega \left[U'(\rho_\infty) - U'(\rho_{k+1})\right]\left(\rho_{k+1} - \rho_k\right) dx \\
&= E(\rho_{k+1}|\rho_\infty) + \tau\int_\Omega \left[U'(\rho_\infty) - U'(\rho_{k+1})\right] \operatorname{div}\left(\rho_k \nabla\left(V + U'(\rho_{k+1})\right)\right) dx \\
&= E(\rho_{k+1}|\rho_\infty) - \tau\int_\Omega \left[\nabla\left(V + U'(\rho_{k+1})\right)\right] \operatorname{div}\left(\rho_k \nabla\left(V + U'(\rho_{k+1})\right)\right) dx,
\end{aligned}$$

where convexity of U, the fact that $\rho_\infty > 0$ under the assumptions of Theorem 2.2 and (8) were used. Integration by parts in the second term using (9) gives

$$\begin{aligned}
-\int_\Omega \left[\nabla\left(V + U'(\rho_{k+1})\right)\right] &\operatorname{div}\left(\rho_k \nabla\left(V + U'(\rho_{k+1})\right)\right) dx \\
&= \int_\Omega \rho_k |\nabla V + U''(\rho_{k+1})\nabla\rho_{k+1}|^2 dx. \\
&= \int_\Omega \rho_{k+1}\frac{\rho_k}{\rho_{k+1}} |\nabla V + U''(\rho_{k+1})\nabla\rho_{k+1}|^2 dx.
\end{aligned}$$

Now, the maximum principle in Theorem 2.2 implies that $0 < \rho_{s,M_1} \le \rho_k \le \rho_{s,M_2}$ for all $k \ge 1$. This together with (13) yields to

$$\left(1 + 2\lambda\kappa\tau\right) E(\rho_{k+1}|\rho_\infty) \le E(\rho_k|\rho_\infty),$$

for all $k \ge 0$, where

$$\kappa := \min_{x\in\bar\Omega} \frac{\rho_{s,M_1}}{\rho_{s,M_2}} > 0.$$

Therefore we conclude that for all $k \ge 1$

$$E(\rho_k|\rho_\infty) \le \left(1 + 2\lambda\kappa\tau\right)^{-k} E(\rho_0, \rho_\infty). \qquad \square$$

The essential prerequisite in Theorem 2.2 and 2.3 is the assumption that the initial data ρ_{k-1} is bounded from below and above by stationary functions which are greater than zero. For some non-linear diffusion equations, like the FDE, i.e. (2) with $0 < m < 1$, this condition is not limiting since it is satisfied for all times. For others like the PME, i.e. (2) with $m > 1$, this is not the case.

2.2. **Finite Element Discretization.** In the following we discuss the finite element solution of (1), more precisely the spatial discretization of system (7). For simplicity we restrict to a two-dimensional setting, but the extension to other dimensions is obvious. Let $\mathcal{T}_h$ denote the regular partition of Ω into triangles T and $\mathcal{E}_h$ the set of element interfaces E. We choose ρ and μ to be in $\mathcal{Q}_h$ and $\mathbf{j} \in \mathcal{V}_h$ given by

$$\mathcal{V}_h = \{\mathbf{q} \in \left[L^2(\Omega)\right]^2 \ : \ \mathbf{q}\mid_T \in RT_0(T) \ \text{ for all } T \in \mathcal{T}_h\}, \tag{14}$$

$$\mathcal{Q}_h = \{v \in L^2(\Omega) \ : \ v\mid_T \in P_0(T) \ \text{ for all } T \in \mathcal{T}_h\}. \tag{15}$$

Here P_j is the space of polynomials of degree $\leq j$ and RT_0 denotes the lowest order Raviart-Thomas element

$$RT_0 = \{\mathbf{q} \in \left[L^2(\Omega)\right]^2 : \mathbf{q}\mid_T = \begin{pmatrix} a \\ b \end{pmatrix} + c\begin{pmatrix} x \\ y \end{pmatrix} \text{ with } a, b, c \in \mathbb{R};$$
$$\mathbf{q} \cdot \eta \text{ continuous across the element interface } E\}.$$

The fully discrete scheme can be written as: Given $\rho_{k-1} \in L^1(\Omega)$ with $0 < c_1 \leq \rho_{k-1}(x) \leq c_2$, find $\rho_k, \mu_k \in \mathcal{Q}_h$ and $\mathbf{j}_k \in \mathcal{V}_h$ with $\mathbf{j}_k \cdot \eta = 0$ on $\partial\Omega$, such that

$$\int_\Omega (U'(\rho_k) + W * \rho_k) w \, dx - \int_\Omega \mu_k w \, dx = -\int_\Omega V w \, dx \qquad \forall w \in \mathcal{Q}_h \tag{16a}$$

$$-\int_\Omega \rho_k \, \xi \, dx + \sqrt{\tau} \int_\Omega \operatorname{div} \mathbf{j}_k \, \xi \, dx = -\int_\Omega \rho_{k-1} \xi \, dx \quad \forall \xi \in \mathcal{Q}_h \tag{16b}$$

$$\sqrt{\tau} \int_\Omega \mu_k \operatorname{div} \mathbf{q} \, dx + \int_\Omega \frac{1}{\max(\rho_{k-1}, h)} \mathbf{j}_k \cdot \mathbf{q} \, dx = 0 \qquad \forall \mathbf{q} \in \mathcal{V}_h. \tag{16c}$$

Note that we replace the term ρ_{k-1}^{-1} by $\max(\rho_{k-1}, h)^{-1}$, where h denotes the maximum mesh size, to ensure the stability. This stabilization allows us to use the numerical scheme (16) for problems, where we cannot guarantee the strict positivity of solutions for all time steps. The existence and uniqueness is straightforward to show:

Theorem 2.4. *Let $0 < c_1 \leq \rho_{k-1} \leq c_2$ almost everywhere in Ω, for some $c_1, c_2 \in \mathbb{R}^+$. Then for $W \equiv 0$ there exists a unique solution of the mixed formulation (16), which further conserves mass, i.e.*

$$\int_\Omega \rho_k \, dx = \int_\Omega \rho_{k-1} \, dx, \tag{17}$$

for any $\tau > 0$. If $W \neq 0$ and $W \in L^1(\mathbb{R}^d)$ there exists a unique solution if τ is sufficiently small.

Proof. The chosen discretization (15), i.e. piecewise constant basis functions for ξ, leads to an exact pointwise relation and allows us to eliminate the variable ρ_k in (16b) . Then the rewritten system (16) is the optimality condition for the minimization of

$$J_k(\mathbf{j}) := E(\rho_{k-1} + \sqrt{\tau}\,\mathrm{div}\,\mathbf{j}) + \frac{1}{2}\int_\Omega \frac{1}{\max(\rho_{k-1}, h)}|\mathbf{j}|^2\,dx, \tag{18}$$

in the set $\mathbf{j} \in \mathcal{V}_h$ where $\mathbf{j}\cdot\eta = 0$. Moreover, we see by divergence theorem that

$$\int_\Omega \rho_k\,dx = \int_\Omega \rho_{k-1}\,dx + \sqrt{\tau}\int_\Omega \mathrm{div}\,\mathbf{j}\,dx = \int_\Omega \rho_{k-1}\,dx$$

due to the continuity of the Raviart Thomas elements (14) with $\mathbf{j}\cdot\eta = 0$.

Since U is nonnegative the internal energy is bounded below by zero, and since ρ_{k-1} is bounded we find

$$\begin{aligned} J_k(\mathbf{j}) \geq\; & c\int_\Omega (\rho_{k-1} + \sqrt{\tau}\,\mathrm{div}\,\mathbf{j})\;V\;dx + C\int_\Omega |\mathbf{j}|^2\,dx \\ & + \frac{1}{2}\int_\Omega (W * (\rho_{k-1} + \sqrt{\tau}\,\mathrm{div}\,\mathbf{j}))(\rho_{k-1} + \sqrt{\tau}\,\mathrm{div}\,\mathbf{j})\,dx. \end{aligned}$$

Applying Young's inequality to the first term and using the fact that the divergence operator is bounded on the finite-dimensional subspace we further obtain

$$\begin{aligned} J_k(\mathbf{j}) \geq\; & c\int_\Omega |\mathbf{j}|^2\,dx - c\int_\Omega |V|^2\,dx \\ & + \frac{1}{2}\int_\Omega (W * (\rho_{k-1} + \sqrt{\tau}\,\mathrm{div}\,\mathbf{j}))(\rho_{k-1} + \sqrt{\tau}\,\mathrm{div}\,\mathbf{j})\,dx, \end{aligned}$$

which already yields a lower bound for $W \equiv 0$. From the properties of the convolution we have for $W \neq 0$

$$\begin{aligned} & \int_\Omega (W * (\rho_{k-1} + \sqrt{\tau}\,\mathrm{div}\,\mathbf{j}))(\rho_{k-1} + \sqrt{\tau}\,\mathrm{div}\,\mathbf{j})\,dx \\ & \qquad \geq -\|W\|_{L^1}\|\rho_{k-1} + \sqrt{\tau}\,\mathrm{div}\,\mathbf{j}\|_{L^2}^2 \geq -C_1 - C_2\tau\int_\Omega |\mathbf{j}|^2\,dx. \end{aligned}$$

If $C_2\tau < c$, i.e. τ sufficiently small, then we conclude again a lower bound on J_k. Since J_k is the sum of convex and a quadratic functional, it is lower semicontinuous and we can conclude the existence of a minimizer.

If $W \equiv 0$, then J_k is a sum of convex terms, with the last one being strictly convex, thus the minimizer is unique. For τ sufficiently small the term $\frac{1}{2}\int_\Omega |\mathbf{j}|^2\,dx$ is again dominating in J_k and one hence obtains strict convexity, which implies the uniqueness of the minimizer. □

Remark 2. We mention that for problems with $W \neq 0$, one obtains a choice of τ of the order of h^2 in the proof of Theorem 2.4. This is however due to the very general assumptions on the interaction term and the nonlinear diffusion, which includes interactions that can lead to an effective behaviour like in a backward

diffusion problem or to finite time blow up. For most practical examples of interaction kernels and nonlinear diffusions, the admissible order of τ to have existence and uniqueness can be significantly increased.

The proof of Theorem 2.4 shows that we can compute the discrete solution by solving a strictly convex variational problem in each time step, which can be realized by a descent method or Newton's method. In many cases even one step of Newton's method, started at the values from the previous time step, is sufficient, as we shall also see for the PME in the next Section.

Finally we are able to show that the maximum principle is conserved:

Theorem 2.5. *Let $\rho_k, \mu_k \in \mathcal{Q}_h$ and $\mathbf{j}_k \in \mathcal{V}_h$ satisfy (16) with $W \equiv 0$, such that $0 < c_1 \leq \mu_{k-1}|_T \leq c_2$ for all triangles T. Then*

$$c_1 \leq \mu_k|_T \leq c_2 \quad \text{for all } T.$$

Proof. Assume there exists a triangle T such that where μ_k is smaller than c_1 and minimal, i.e. $\mu_k(x) < c_1$ for all $x \in T$ and $\mu_k|_T \leq \mu_k|_{\tilde{T}}$ for all triangles $\tilde{T}$. The chosen discretization (15), i.e. piecewise constant basis functions w, leads to a pointwise relation in (16a). Therefore we conclude with the monotonicity of U' that

$$\operatorname{div} \mathbf{j}_k = \frac{\rho_k - \rho_{k-1}}{\tau} = \frac{(U')^{-1}(\mu_k - V) - (U')^{-1}(\mu_{k-1} - V)}{\tau} < 0$$

in the triangle T. Let us now consider any adjacent $\tilde{T}$ and its common edge E and midpoint M. We choose the Raviart-Thomas basis function satisfying

$$\mathbf{q} \cdot \eta = \begin{cases} 1 & \text{for } x \in E \\ 0 & \text{elsewhere.} \end{cases}$$

For $\mathbf{q} \in RT_0$ and μ being a piecewise constant function the following holds (due to exactness of quadrature in the midpoints of the edges) for an appropriate weighted harmonic mean $\bar{\rho}_{k-1}$ of $\max\{\rho_{k-1}, h\}$:

$$\begin{aligned}
\frac{\mathbf{j}_k \cdot \eta}{\bar{\rho}_{k-1}} |_M &= -\left(\int_T \mu \,|_T \operatorname{div} \mathbf{q} \, dx + \int_{\tilde{T}} \mu \,|_{\tilde{T}} \operatorname{div} \mathbf{q} \, dx \right) \\
&= -\left(\mu \,|_T \int_T \operatorname{div} \mathbf{q} \, dx + \mu \,|_{\tilde{T}} \int_{\tilde{T}} \operatorname{div} \mathbf{q} \, dx \right) \\
&= -\left(\mu \,|_T \int_{\partial T} \mathbf{q} \cdot \eta \, ds + \mu \,|_{\tilde{T}} \int_{\partial \tilde{T}} \mathbf{q} \cdot \eta \, ds \right) \\
&= -\left(\mu \,|_T \int_E \mathbf{q} \cdot \eta \, ds - \mu \,|_{\tilde{T}} \int_E \mathbf{q} \cdot \eta \, ds \right),
\end{aligned}$$

where the negative sign in the second term arises from the different orientation of the normal to E on $\partial \tilde{T}$. Thus,

$$\int_E \mathbf{j}_k \cdot \eta \, ds = |E| \, \mathbf{j}_k \cdot \eta \,|_M = -c \, (\mu \,|_T - \mu \,|_{\tilde{T}}) \geq 0.$$

Taking into account that the previous estimates are valid for all adjacent triangles and if there are boundary edges they do not have contribution due to the boundary condition $\mathbf{j}_k \cdot \eta = 0$, we have

$$\int_{\partial T} \mathbf{j}_k \cdot \eta \, ds \geq 0.$$

But since $\operatorname{div} \mathbf{j}_k < 0$

$$0 \leq \int_{\partial T} \mathbf{j}_k \cdot \eta \, ds = \int_T \operatorname{div} \mathbf{j}_k \, dx < 0,$$

leading to a contradiction. □

3. Porous Medium and Fast Diffusion Equation

In this Section we apply the proposed semi-implicit scheme to the PME and the FDE. The PME and FDE on a bounded domain $\Omega \subset \mathbb{R}^2$ are given by

$$\begin{aligned} \frac{\partial \rho}{\partial t} &= \operatorname{div}\left(\nabla \rho^m\right) = \operatorname{div}\left(\frac{m}{m-1} \rho \nabla \rho^{m-1}\right) \\ \rho(x,0) &= \rho_0(x) > 0, \end{aligned} \tag{19}$$

with no flux boundary conditions. We reiterate that the PME equation can be written in the formalism of (5) with the internal energy U given by (2). The different names for $m < 1$ and $m > 1$ are motivated by the distinct behavior of solutions in either case.

There are a number of physical applications, mainly to model fluid flow, heat transfer or diffusion. One famous application is the description of an isentropic gas through a porous medium independently published by Leibenzon and Muskat around 1930. For an extensive overview on the theory of (19) we refer to the books by Vazquez [45, 44]. A fundamental solution of (19) for $m > 1$ was obtained by Zel'dovich, Kompaneets and Barenblatt [4] around 1950. The solution was subsequently found by Pattle in 1959, see [41]. This family of self-similar solutions is given by

$$\mathcal{U}(x,t) = t^{-\alpha} \left(C - k|x|^2 t^{-2\beta}\right)_+^{\frac{1}{m-1}}, \tag{20}$$

where $u_+ = \max(u, 0)$ and

$$\alpha = \frac{d}{d\,(m-1)+2}, \quad \beta = \frac{\alpha}{d}, \quad k = \frac{\alpha\,(m-1)}{2md}. \tag{21}$$

Solutions of the form (20) are often referred to as the *Barenblatt-Pattle (BP) solutions*. The free parameter $C > 0$ can be chosen arbitrarily, but determines the total mass $M = \int_\Omega \mathcal{U} dx$ (or vice versa). The class of self-similar solutions can be easily extended to the FDE, but only in the range $m_c < m < 1$, cf. [35] with

$$m_c = 0 \quad \text{for} \quad d = 1, 2 \quad m_c = \frac{d-2}{d} \quad \text{for} \quad d \geq 3.$$

In principle the formula is the same, except for $m-1$ and k being negative numbers. More precisely we have

$$\mathcal{U}_m(x,t) = t^{-\alpha} F\left(x t^{\frac{\alpha}{d}}\right) \qquad \text{with } F(\xi) = \left(C + \kappa_1 \xi^2\right)^{-\frac{1}{1-m}}, \tag{22}$$

with α given by (21) and $\kappa_1 = -\kappa = \frac{(1-m)\alpha}{2md}$. For $m > 1$ the BP profiles have a compact support, for $m < 1$ the solutions are always positive and decay polynomially at infinity.

3.1. **Numerical Discretization.** In section 2 we presented a semi-implicit time discretization based on the optimal transport formulation of the nonlinear diffusion problem (1). We will apply this approach to the PME (19) and perform an additional linearization step to obtain a symmetric linear scheme. Let ρ_{k-1} denote the solution at time $t = t_{k-1}$. The Lagrange multiplier μ (7) is given by

$$\begin{aligned}\mu &= \frac{m}{m-1}\rho^{m-1} \\ &\approx \frac{m}{m-1}\left(\left(\rho_{k-1}\right)^{m-1} + (m-1)\left(\rho_{k-1}\right)^{2-m}\left(\rho - \rho_{k-1}\right)\right)\end{aligned}$$

and the flux $\mathbf{j} = \rho_{k-1}\nabla\mu$. This linearization results in the following symmetric mixed formulation

$$m\left(\rho_{k-1}\right)^{m-2}\rho - \mu = -\frac{m(2-m)}{m-1}\left(\rho_{k-1}\right)^{m-1} \tag{23a}$$

$$-\rho + \sqrt{\tau}\,\operatorname{div}\mathbf{j} = -\rho_{k-1} \tag{23b}$$

$$-\sqrt{\tau}\nabla\mu + \frac{1}{\rho_{k-1}}\mathbf{j} = 0. \tag{23c}$$

with time steps $\tau = t_k - t_{k-1}$. The corresponding weak formulation is given by: Find $\rho, \mu \in L^2(\Omega)$ and $\mathbf{j} \in H(\operatorname{div}, \Omega)$ such that

$$\int_\Omega m\left(\rho_{k-1}\right)^{m-2}\rho\omega\,dx - \int_\Omega \mu\omega\,dx = -\int_\Omega f\omega\,dx \qquad \forall \omega \in L^2(\Omega) \tag{24a}$$

$$-\int_\Omega \rho\xi\,dx + \int_\Omega \sqrt{\tau}\,\operatorname{div}\mathbf{j}\xi\,dx = -\int_\Omega \rho_{k-1}\xi\,dx \qquad \forall \xi \in L^2(\Omega) \tag{24b}$$

$$\int_\Omega \sqrt{\tau}\mu\,\operatorname{div}\mathbf{q}\,dx + \int_\Omega \frac{1}{\rho_{k-1}}\mathbf{j}\cdot\mathbf{q}\,dx = 0 \qquad \forall \mathbf{q} \in H(\operatorname{div}, \Omega), \tag{24c}$$

with $f = \frac{m(2-m)}{m-1}\left(\rho_{k-1}\right)^{m-1}$. Using the classical theory of mixed finite element methods (cf. [12]) we can verify the following existence and uniqueness result:

Theorem 3.1. *If $0 < c_1 \le \rho_{k-1}(x) \le c_2$ for some $c_1, c_2 \in \mathbb{R}^+$, then mixed formulation (24) has a unique solution.*

Proof. System (24) can be written as (eliminating the variable ρ)

$$a(\mathbf{j}, \mathbf{q}) + b(\mathbf{q}, \mu) = 0 \qquad \text{and} \qquad b(\mathbf{j}, \xi) - c(\mu, \xi) = g(\xi)\,.$$

Under the assumption made above we can show that the bilinear form a is bounded and coercive, b is bounded and satisfies the inf-sup condition,

$$\exists\ \beta_1 > 0 \qquad \sup_{\substack{\mathbf{q}\in H(\mathrm{div},\Omega)\\ v\neq 0}} \frac{b(\mathbf{q},\mu)}{\|\mathbf{q}\|_{H(\mathrm{div},\Omega)}} \geq \beta_1 \|\mu\|_{L^2(\Omega)} \qquad \forall \mu \in L^2(\Omega),$$

and c is bounded and coercive. Therefore system (24) admits a unique solution. □

System (24) can be discretized using the finite element discretization proposed in Section 2.2. Given $\rho_{k-1} \in L^2(\Omega)$ with $0 < c_1 \leq \rho_{k-1}(x) \leq c_2$, we look for $\rho_k, \mu_k \in \mathcal{Q}_h$ and $\mathbf{j}_k \in \mathcal{V}_h$ with $\mathbf{j}_k \cdot n = 0$ on $\partial\Omega$, such that

$$\text{(25a)} \qquad \int_\Omega m\left(\rho_{k-1}\right)^{m-2} \rho_k w \, dx - \int_\Omega \mu_k w \, dx = \int_\Omega f(\rho_{k-1}) w \, dx \qquad \forall w \in \mathcal{Q}_h$$

$$\text{(25b)} \qquad -\int_\Omega \rho_k \xi \, dx + \sqrt{\tau} \int_\Omega \operatorname{div} \mathbf{j}_k \xi \, dx = -\int_\Omega \rho_{k-1} \xi \, dx \qquad \forall \xi \in \mathcal{Q}_h$$

$$\text{(25c)} \qquad \sqrt{\tau} \int_\Omega \mu_k \operatorname{div} \mathbf{q} \, dx + \int_\Omega \frac{1}{\rho_{k-1}} \mathbf{j}_k \cdot \mathbf{q} \, dx = 0 \qquad \forall \mathbf{q} \in \mathcal{V}_h.$$

Existence and uniqueness is also guaranteed for the fully discrete scheme (25) We reiterate that we replace the term ρ_{k-1}^{-1} by $\max(\rho_{k-1}, h)^{-1}$, where h denotes the maximum mesh size to ensure the stability. In addition we are able to show the following maximum principle in analogous way to Theorem 2.2.

Theorem 3.2. *Let $\rho, \mu \in \mathcal{Q}_h$ and $\mathbf{j} \in \mathcal{V}_h$ satisfying (25). Let all assumptions of Theorem 3.1 hold. Then*

$$c_1 \leq \rho(x) \leq c_2 \quad \text{for all } x \in \Omega.$$

3.2. **Numerical Experiments.** Finally we would like to illustrate the behavior of the proposed numerical scheme with computational experiments. All numerical results in this and the next section are calculated using the finite element code Netgen/NgSolve of J. Schöberl, cf. [42].

We choose Ω to be a circle of radius $r = 2$, which has been decomposed into 13010 triangles with maximum mesh size $h = 0.05$. The initial datum is set to the Barenblatt-Pattle solution (20) at time $t = \tau$. We reiterate that we replace ρ_{k-1} in ρ_{k-1}^{-1} and $(\rho_{k-1})^{m-2}$ by $\max(\rho_{k-1}, h)$, where h equals the maximum mesh size.

As long as the solution support does not touch the boundary, the solution in the bounded domain with Neumman boundary condition coincides with the self-similar BP solution and thus, we can compare the approximated solution of our scheme to the exact BP solution. The solution for $m = 3$ is illustrated in figure 1 as well as the difference of the approximate solution ρ_h to the BP solution in the L^∞-Norm.

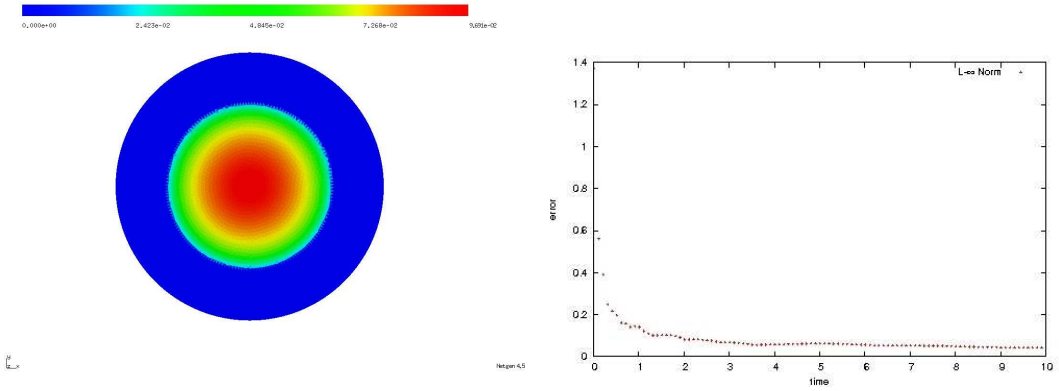

(a) $t = 10$ (b) Difference of the approximated solution to the BP solution in L^∞-Norm

FIGURE 1. Density ρ at $t = 10$ and difference in L^∞-Norm to the BP solution for $m = 3$.

Figure 2 shows the solution and the error for $m = 5$. Note that the approximate solution has a compact support and that the slope of the solution at the boundary of its support is becoming steeper for greater values of m.

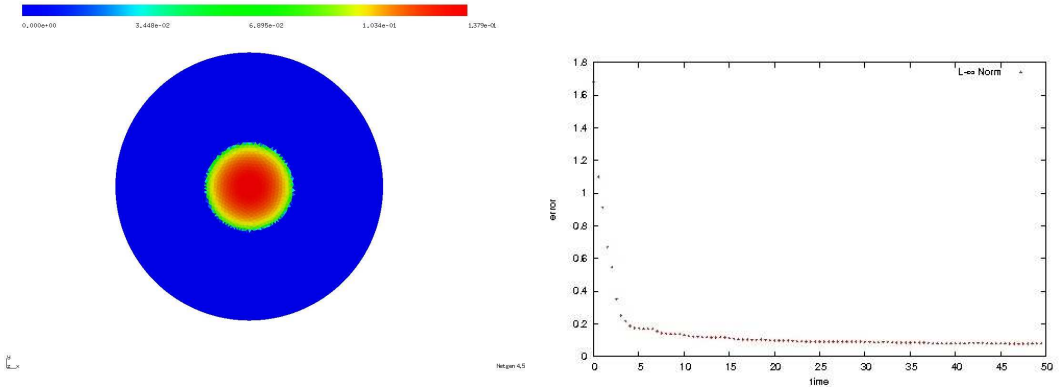

(a) $t = 50$ (b) Difference of the approximated solution to the BP solution in L^∞-Norm

FIGURE 2. Density ρ at $t = 50$ and difference in L^∞-Norm to the BP solution for $m = 5$.

Next we consider the solution of the nonlinear Fokker-Planck equation (FPE)

$$\frac{\partial \rho}{\partial t} = \operatorname{div}(\nabla \rho^m + x\rho) \tag{26}$$

where $m = 2$. This equation is of particular interest since there exists a time dependent scaling which transform (26) into the PME (19). One can easily check

that the compactly supported equilibrium solution of (26) coincides with the BP solution (20) at time $t = 1$. The solution of the nonlinear FPE, as well as the evolution of the difference between ρ and the BP-profile at $t = 1$ is depicted in figure 3.

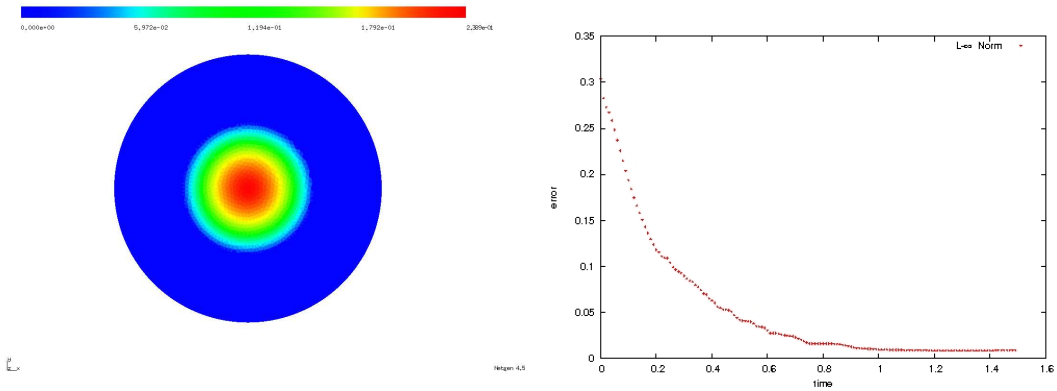

(a) $t = 1.5$

(b) Difference of the approximated solution to the BP solution at $t = 1$in L^∞-Norm

FIGURE 3. Density ρ at $t = 1.5$ and difference in L^∞-Norm to the BP solution for the nonlinear FPE (26).

Our final example illustrates the behavior for solutions of fast diffusion equations. Note that in case of fast diffusion, i.e. $m < 1$ the BP profiles do not have a compact support. The presented numerical scheme is mass conserving, therefore it is not possible to measure the difference of the approximated solution to the Barenblatt solution on a bounded domain. The evolution of the solution for $m = 0.8$ is illustrated in figure 4. As implied by the name, the solutions of the fast diffusion equation spread out very fast and converge rapidly to a constant value due to the Neumann boundary conditions.

4. Chemotaxis: The Patlak-Keller-Segel model

In this section we consider the simplified PKS model on the bounded domain $\Omega \subset \mathbb{R}^2$ (cf. [17]),

$$\frac{\partial \rho}{\partial t} = \operatorname{div}\left(\kappa \nabla \rho - \chi \rho \nabla v\right) \tag{27a}$$

$$-\Delta v = \rho - \langle \rho \rangle \tag{27b}$$

$$\rho(x, 0) = \rho_0 \geq 0,$$

with homogenous Neumann boundary conditions. The total mass of cells is conserved through the evolution:

$$M := \int_\Omega \rho_0 \, dx = \int_\Omega \rho \, dx.$$

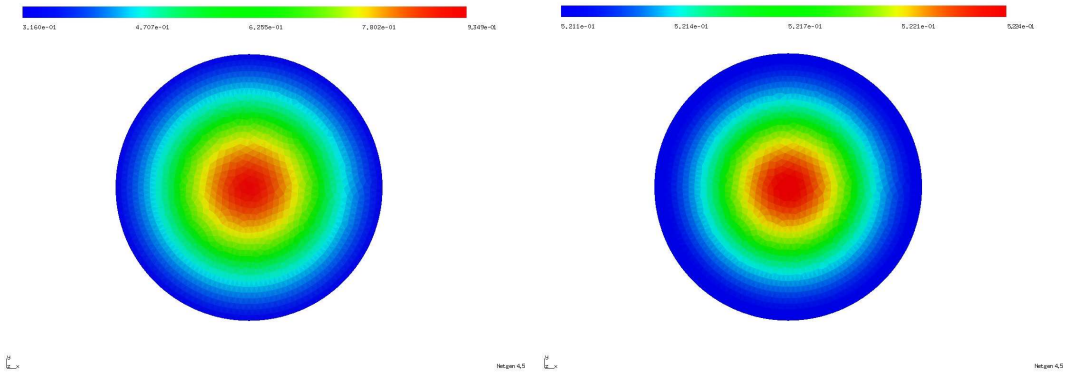

(a) $t = 1$ (b) $t = 3$

FIGURE 4. Density ρ at $t = 1$ and $t = 3$ in case of the FDE with $m = 0.8$.

This model is a gradient flow for the energy

$$E(\rho) = \inf_v \int_\Omega \left(\frac{\kappa}{\chi}\rho \log \rho + \frac{1}{2}|\nabla v|^2 - \rho v + \langle\rho\rangle v\right) dx \tag{28}$$

It is well know that solution of the PKS system (27) may blow up in time, depending on the spatial dimension and the total mass M. In spatial dimension one solutions exist global in time. In spatial dimension two the total mass of the system determines whether the solution exist global in time or blow up, in dimension three the problem the solutions always blow up in finite time. In [33] Jäger and Luckhaus presented first results, further results for the two-dimensional PKS system have been derived for the whole domain $\mathbb{R}^2$ in [25, 11, 10, 26] and for bounded domains $\Omega \subset \mathbb{R}^2$ in [17, 30]. For a detailed presentation of various aspects and results for the PKS model we refer to [31]. In case of the simplified PKS model (27), solutions blows up in finite time if $\frac{\chi M}{\kappa} > \mathcal{C}$ with

$$\mathcal{C} = \begin{cases} 8\pi & \text{if } \Omega = \mathbb{R}^2 \\ 4\pi & \text{if } \Omega \text{ is a } C^2\text{, bounded, connected domain,} \end{cases}$$

cf. [17]. Theoretical results on the behavior of solution after blow-up have been presented by Dolbeault and Schmeiser in [26]. Another interesting extension of the PKS model has been studied in [17], namely a PKS system with nonlinear porous medium type diffusion given by

$$\frac{\partial \rho}{\partial t} = \operatorname{div}\left(\nabla \rho^m - \chi \rho \nabla v\right) \tag{29a}$$

$$-\Delta v = \rho, \tag{29b}$$

with the energy

$$E(\rho) = \inf_v \int_\Omega \left(\frac{1}{m+1}\rho^{m+1} + \frac{1}{2}|\nabla v|^2 - \rho v\right)\, dx. \tag{30}$$

Here solutions behave quite differently, with no finite time blow up occurring. We will also observe this behavior in our numerical simulations.

We apply the linearization presented in section 2 to solve (27) and investigate numerically the occurrence of blow up solutions. Following the notions of section 2 we introduce the new variable $\mu = \log \rho \approx \log \rho_{k-1} + \frac{1}{\rho_{k-1}}(\rho_k - \rho_{k-1})$ and $\mathbf{j} = \rho \nabla \mu$ and obtain the weak formulation of (27): Find $v, \rho_k, \mu_k \in L^2(\Omega)$ and $\mathbf{e}, \mathbf{j}_k \in H(\mathrm{div}, \Omega)$ such that

$$\begin{aligned}
\int_\Omega \mathbf{e}\cdot\mathbf{p}\, dx - \int_\Omega v \,\mathrm{div}\,\mathbf{p}\, dx &= 0 && \forall \mathbf{e} \in H(\mathrm{div},\Omega)\\
-\int_\Omega \mathrm{div}\,\mathbf{e} r\, dx + \int_\Omega \rho_k r\, dx &= -\int_\Omega \langle\rho_0\rangle r\, dx && \forall r \in L^2(\Omega)\\
\int_\Omega \chi v w\, dx - \int_\Omega \frac{\rho_k}{\rho_{k-1}} w\, dx + \int_\Omega \mu_k w\, dx &= \int_\Omega f w\, dx && \forall w \in L^2(\Omega)\\
\int_\Omega \rho_k \xi\, dx - \int_\Omega \sqrt{\tau}\,\mathrm{div}\,\mathbf{j}_k \xi\, dx &= \int_\Omega \rho_{k-1}\xi\, dx && \forall \xi \in L^2(\Omega)\\
\int_\Omega \sqrt{\tau}\mu_k \,\mathrm{div}\,\mathbf{q}\, dx - \int_\Omega \frac{1}{\rho_{k-1}}\mathbf{j}_k\cdot\mathbf{q}\, dx &= 0 && \forall \mathbf{q} \in H(\mathrm{div},\Omega),
\end{aligned}$$

where $f = (\log \rho_{k-1} + 1)$. We use the same discretization as in the previous section, namely $\mathbf{e}$ and $\mathbf{q}$ in $\mathcal{V}_h$ and v, ρ_k and μ_k in $\mathcal{Q}_h$. Again existence and uniqueness can be guaranteed for $\rho_{k-1}(x) > 0$. We will now illustrate the blow up behavior of the simplified PKS model (27) with various numerical examples. We choose a Gaussian as initial distribution

$$\rho_0(x,y) = \frac{M}{\sqrt{2\pi}} e^{-\frac{(x-x_0)^2+(y-y_0)^2}{2}},$$

where M denotes the total initial mass. The test geometry is a square of size $[-5,5]\times[-5,5]$ with a discretization of 10348 triangles. To increase the accuracy of our method and observe the blow up behavior of the solution as long as possible, we use an h-refinement technique at the corners of the domain, where we expect the blow up to happen.

As a first example we choose a radially symmetric initial distribution with $x_0 = y_0 = 0$ and $M = 10\pi$. Figure 5 shows the expected blow up at the center of the domain.

In case of a non radially symmetric initial Gaussian with $x_0 = 2.5$, $y_0 = -2.5$ and $M = 10\pi$, the blow up happens at the boundary of the domain, see Figure 6. For non radially symmetric initial masses which satisfies

$$4\pi < c < 8\pi$$

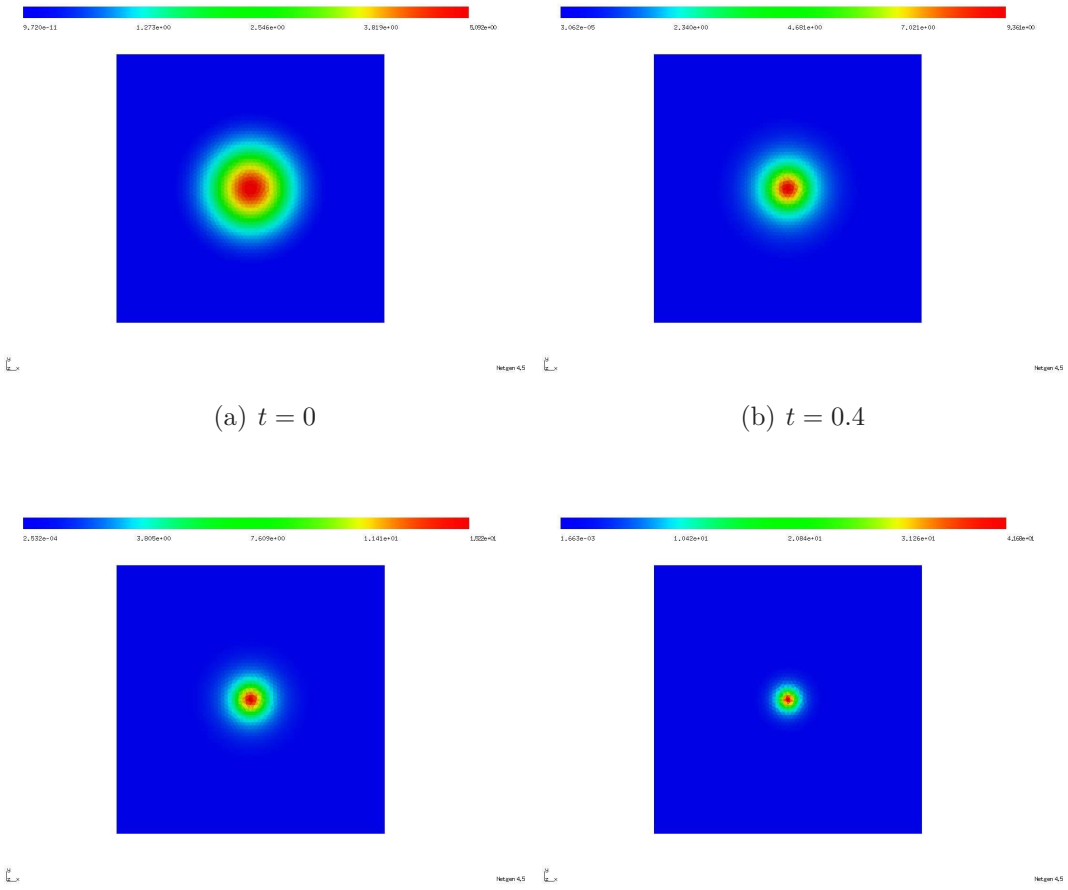

(a) $t = 0$ (b) $t = 0.4$

(c) $t = 0.8$ (d) $t = 1.5$

FIGURE 5. Evolution of the density ρ with symmetric initial guess and mass $M = 10\pi$.

the blow up has to happen at the boundary. Again we choose a Gaussian with $x_0 = y_0 = 2.5$ and initial mass $M = 5\pi$ as an initial guess. The expected blow up behavior is depicted in Figure 7. We would like to mention that in case of the simplified PKS system (27) with Dirichlet boundary conditions for v, the blow up always happens in the center of mass. Our numerical simulations support this statement and agree with the results by Filbet [27] and Morocco [37].

In our final example we consider the PKS model with degenerate diffusion (29) where $m = 3$. The initial mass is set to one. Here the solution converges quickly to a stationary profile, similar to the Barenblatt solution, see figure 8. Such an equilibration result is not proved theoretically in the literature but expected for all masses in the Cauchy problem without Neumann-boundary condition. In addition we do not observe the blow-up behavior for large initial mass as in the case of the simplified PKS model (27). The diffusion term is dominating,

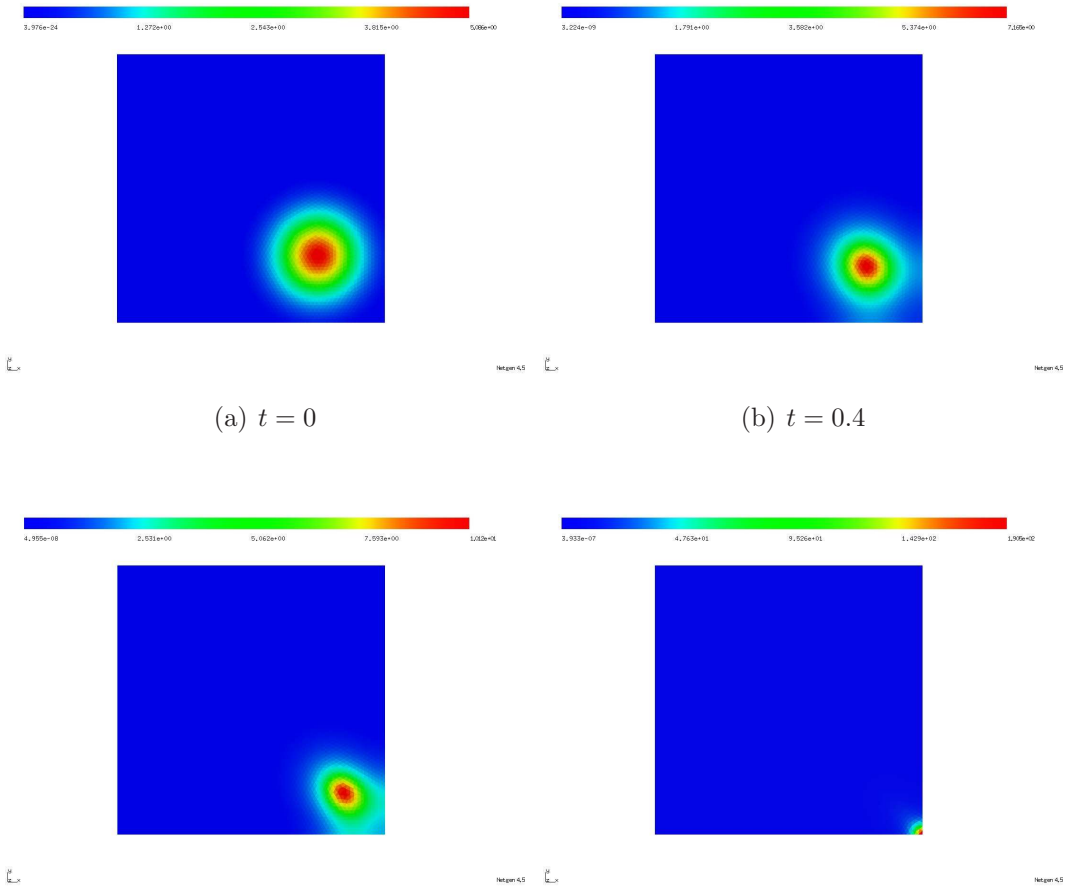

(a) $t = 0$ (b) $t = 0.4$

(c) $t = 0.8$ (d) $t = 1.4$

FIGURE 6. Evolution of the density ρ with non symmetric initial guess and mass $M = 10\pi$.

therefore solutions flatten out quickly and go to a constant profile once they touch the boundary.

5. External Velocities and Stabilization

We finally want to comment on the extension of the scheme to situations as in hydrodynamics, where an additional velocity field of non-gradient structure appears in the equation, i.e.,

$$\frac{\partial \rho}{\partial t} = \operatorname{div}\left(\rho \nabla \left(U'(\rho) + V + W * \rho\right) + \rho u_*\right) \qquad t > 0,\ x \in \mathbb{R}^d, \tag{31}$$

In this case it is natural to split the energy term and the additional convective one before carrying out the linearization of the transport problem and the spatial discretization. Choosing an explicit time stepping for the convective part, we end

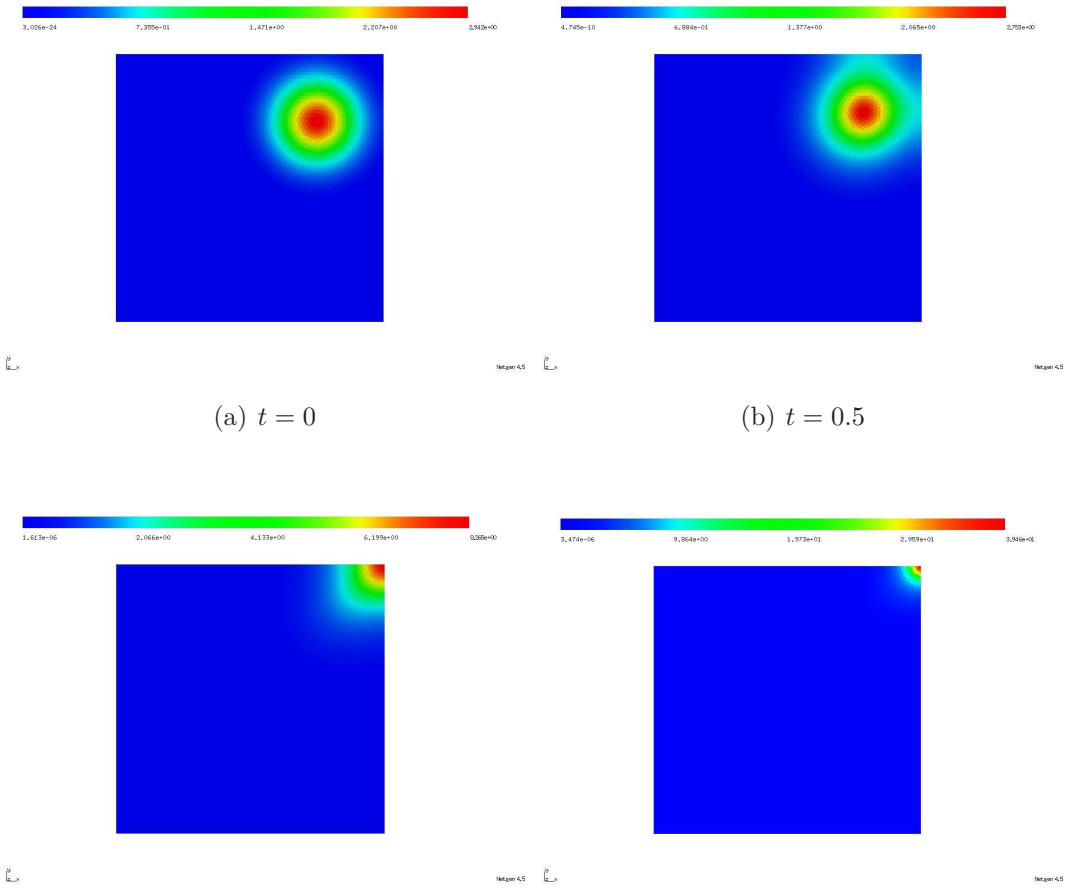

(a) $t = 0$ (b) $t = 0.5$

(c) $t = 1.5$ (d) $t = 2$

FIGURE 7. Evolution of the density ρ with non symmetric initial guess and mass $M = 6\pi$.

up with the linearized optimal transport problem Given a density ρ_{k-1}, find ρ_k, ρ and u such that

$$\inf_{\rho,\rho_k,u} \left\{ E(\rho_k) + \int_{t_{k-1}}^{t_k} \int_{\mathbb{R}^d} \frac{|u|^2}{2} \rho_{k-1} dx dt \right\},$$

under the constraint that

$$\begin{aligned} &\frac{\partial \rho}{\partial t} + \operatorname{div}\left(\rho_{k-1}(u - u_*)\right) = 0, \\ &\rho(\cdot, t_{k-1}) = \rho_{k-1}, \quad \rho(\cdot, t_k) = \rho_k, \end{aligned}$$

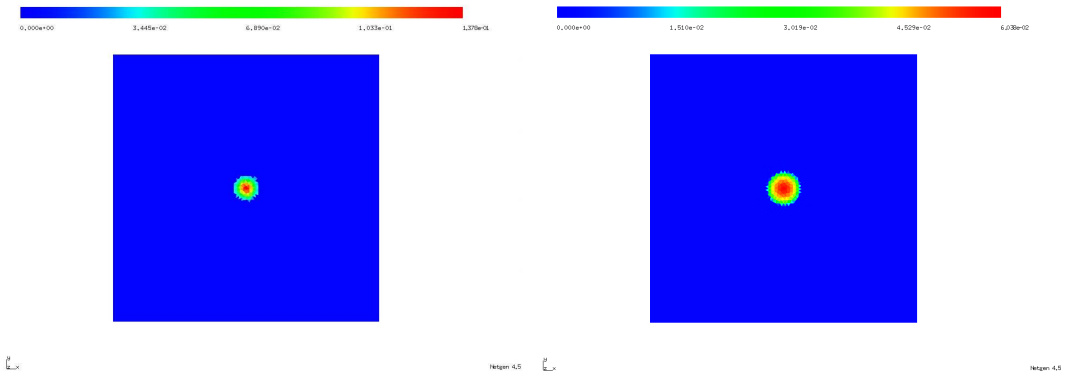

(a) $t = 0$ (b) $t = 20$

FIGURE 8. Evolution a density ρ with masses $m = 1$ with degenerate diffusion.

is satisfied. The corresponding Lagrange functional $\mathcal{L}$ is given by

$$\mathcal{L} = E(\rho_k) + \int_{t_{k-1}}^{t_k} \int_{\mathbb{R}^d} \left[\frac{|u|^2}{2} \rho_{k-1}(x) - \frac{\partial \mu}{\partial t} \rho - \rho_{k-1} \nabla \mu \cdot (u - u_*) \right] dx dt$$
$$- \int_{\mathbb{R}^d} \left[\mu(x, t_{k-1}) \rho_{k-1} - \mu(x, t_k) \rho_k \right] dx,$$

and the optimality conditions remain the same as in Section 2.1, i.e. (7). Then we simply obtain a semidiscrete scheme

$$\frac{\rho_k - \rho_{k-1}}{\tau} = \operatorname{div} \left(\rho_{k-1} \nabla \left(U'(\rho_k) + V \right) + \rho_{k-1} u_* \right), \tag{32}$$

In the mixed finite element discretization (16) only (16b) needs to be changed to

$$- \int_\Omega \rho_k \xi \, dx + \sqrt{\tau} \int_\Omega \operatorname{div} \mathbf{j}_k \xi \, dx = - \int_\Omega \rho_{k-1} \xi \, dx - \tau \ell_{k,*}(\xi) \qquad \forall \xi \in \mathcal{Q}_h, \tag{33}$$

where $\ell_{k,*}(\xi)$ is an appropriate approximation of

$$\int_\Omega \operatorname{div}(\rho_{k-1} u_*) \xi \, dx.$$

Noticing that ξ is a piecewise constant, we find

$$\int_\Omega \operatorname{div}(\rho_{k-1} u_*) \xi \, dx = \sum_T \xi|_T \int_T \operatorname{div}(\rho_{k-1} u_*) \, dx.$$

Thus, the stabilization of this term is exactly the same problem as in any finite volume scheme, a task which is very well understood.

As an example we only present a simple upwinding technique for the case of u_* being defined in the triangle midpoints. For ρ_{k-1} continuous one would have

$$\sum_T \xi|_T \int_T \operatorname{div}(\rho_{k-1}u_*)\ dx = \sum_T \xi|_T \int_{\partial T} \rho_{k-1}u_* \cdot \eta\ ds.$$

In order to rewrite the problem as an integration over edges, we choose an order for each edge and its normal, and denote the triangle into which the normal points by $T^+(E)$ and the second triangle adjacent to this edge by $T^-(E)$. Then

$$\sum_T \xi|_T \int_{\partial T} \rho_{k-1}u_* \cdot \eta\ ds = \sum_E \int_E \rho_{k-1}u_* \cdot \eta\ ds(\xi|_{T^-(E)} - \xi|_{T^+(E)}).$$

For the piecewise constant discretization the value of ρ_{k-1} in the integral over E has to be approximated from the values in the adjacent triangles. We choose the upwind direction based on the flow direction $-u_* \cdot \eta$, which gives

$$\begin{aligned}\ell_*(\xi) = &\sum_{E, u_*\cdot\eta<0} \int_E u_* \cdot \eta\ ds \rho_{k-1}|_{T^+(E)}(\xi|_{T^-(E)} - \xi|_{T^+(E)}) + \\ &\sum_{E, u_*\cdot\eta>0} \int_E u_* \cdot \eta\ ds \rho_{k-1}|_{T^-(E)}(\xi|_{T^-(E)} - \xi|_{T^+(E)}).\end{aligned} \tag{34}$$

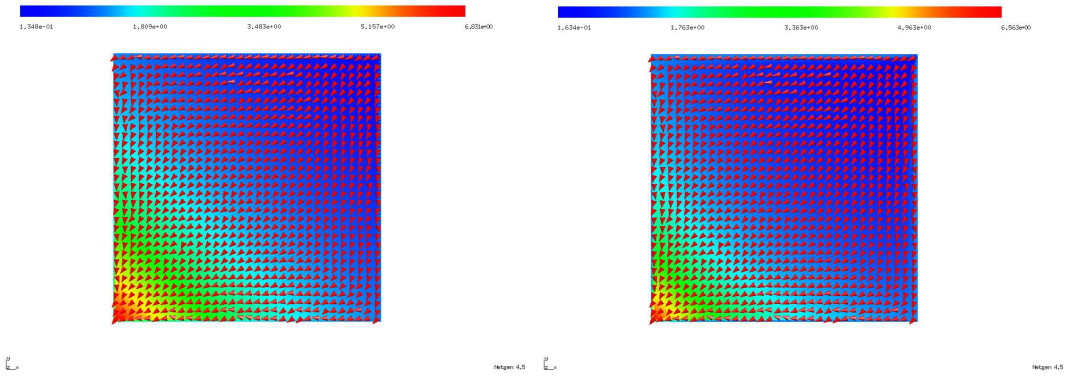

(a) Without upwind (b) With upwind

FIGURE 9. Solution of (35) with no upwind (left) and upwind (right).

In order to test this approach computationally, we investigate the example

$$\begin{aligned}\frac{\partial \rho}{\partial t} &= \operatorname{div}(\varepsilon \nabla \rho + \rho u_*) \\ \rho(x,t) &= 1 \qquad \text{for all } x \in \partial\Omega\end{aligned} \tag{35}$$

with $\rho(x,0) = 1$, $\varepsilon = 10^{-5}$ and $u_* = (x(x-1), y(y-1))$ (satisfying $u_* \cdot \eta = 0$ on the boundary $\partial\Omega$). The domain $\Omega = [0,1] \times [0,1]$ is decomposed into 6972

triangles, the time steps $\tau = 10^{-2}$. The solution at time $t = 1$ and the velocity field u_* is depicted in Figure 9. The proposed upwind scheme is mass preserving and resolves the boundary layer much better than the standard discretization.

Acknowledgments

JAC was partially supported by MTM2008-06349-C03-03 project DGI-MCI (Spain) and 2009-SGR-345 from AGAUR-Generalitat de Catalunya. MTW acknowledges support by Award No. KUK-I1-007-43, made by King Abdullah University of Science and Technology (KAUST). We acknowledge the Institute for Pure and Applied Mathematics (University of California, Los Angeles), the International Center for Mathematical Sciences (Edinburgh, UK), the Centro de Ciencias de Benasque and CRM (Barcelona) for their kind hospitality in several stages of this work.

References

[1] L. Ambrosio, N. Gigli, and G. Savaré. *Gradient Flows in Metric Spaces and in the Space of Probability Measures*. Lectures in Mathematics ETH Zürich. Birkhäuser Verlag, Basel, 2005.

[2] A. Arnold, P. Markowich, G. Toscani, and A. Unterreiter. *On convex Sobolev inequalities and the rate of convergence to equilibrium for Fokker-Planck type equations*, Comm. Partial Differential Equations, **26 (1-2)** (2001),43–100.

[3] A. Arnold and A. Unterreiter. *Entropy decay of discretized Fokker-Planck equations. I. Temporal semidiscretization*, Comput. Math. Appl., **46 (10-11)** (2003), 1683–1690.

[4] G. I. Barenblatt. *On some problems of unsteady filtration*, Izv. Akad. Nauk SSSR. Otd. Tehn. Nauk , **6** (1954), 97–110.

[5] J.-D. Benamou and Y. Brenier. *A computational fluid mechanics solution to the Monge-Kantorovich mass transfer problem*, Numer. Math., **84(3)** (2000), 375–393.

[6] D. Benedetto, E. Caglioti, and M. Pulvirenti. *A kinetic equation for granular media*. RAIRO Modél. Math. Anal. Numér., **31** (1997), 615–641.

[7] D. Benedetto, E. Caglioti, J.A. Carrillo, and M. Pulvirenti. *A non-maxwellian steady distribution for one-dimensional granular media*, J. Stat. Phys., **91** (1998),979-990.

[8] A. Bertozzi, J.A. Carrillo, and T. Laurent. *Blowup in multidimensional aggregation equations with mildly singular interaction kernels*. Nonlinearity, **22** (2009), 683-710.

[9] A. Blanchet, V. Calvez, and J.A. Carrillo. *Convergence of the mass-transport steepest descent scheme for the subcritical Patlak-Keller-Segel model*. SIAM J. Numer. Anal., **46** (2008), 691–721.

[10] A. Blanchet, J. A. Carrillo, and N. Masmoudi. *Infinite time aggregation for the critical PKS model in* $\mathbb{R}^2$. Comm. Pure and Applied Mathematics, **61** (2008), 1449–1481.

[11] A. Blanchet, J. Dolbeault, and B. Perthame. *Two-dimensional Keller-Segel model: optimal critical mass and qualitative properties of the solutions*. Electron. J. Differential Equations, (2006), 44-76.

[12] F. Brezzi and M. Fortin. *Mixed and Hybrid Finite Element Methods*, volume 15 of *Springer Series in Computational Mathematics*. Springer-Verlag, New York, 1991.

[13] C. Budd, R. Carretero-González, and R. Russell. *Precise computations of chemotactic collapse using moving mesh methods*. J. Comput. Phys., **202(2)** (2005), 463–487.

[14] M. Burger, V. Capasso, and D. Morale. *On an aggregation model with long and short range interactions*. Nonlinear Anal., Real World Appl., **8(3)** (2007), 939–958.

[15] M. Burger and M. Di Francesco. *Large time behavior of nonlocal aggregation models with nonlinear diffusion.* Netw. Heterog. Media, **3(4)** (2008), 749–785.
[16] M. Burger, R. S. Eisenberg, and H. W. Engl. *Inverse problems related to ion channel selectivity.* SIAM J. Appl. Math., **67(4)** (2007), 960–989.
[17] V. Calvez and J. A. Carrillo. *Volume effects in the Keller-Segel model: energy estimates preventing blow-up.* J. Math. Pures Appl. (9), **86(2)** (2006), 155–175.
[18] J. A. Carrillo and J. Moll. *Numerical simulation of diffusive and aggregation phenomena in nonlinear continuity equations by evolving diffeomorphisms.* SIAM J. Sci. Computing, (2010). to appear.
[19] J. A. Carrillo, M. Di Francesco, and M. P. Gualdani. *Semidiscretization and long-time asymptotics of nonlinear diffusion equations.* Commun. Math. Sci., **5(suppl. 1)** (2007), 21–53.
[20] J. A. Carrillo, A. Jüngel, P. A. Markowich, G. Toscani, and A. Unterreiter. *Entropy dissipation methods for degenerate parabolic problems and generalized Sobolev inequalities.* Monatsh. Math., **133(1)** (2001), 1–82.
[21] J.A. Carrillo, R.J. McCann, and C. Villani. *Kinetic equilibration rates for granular media and related equations: entropy dissipation and mass transportation estimates.* Rev. Matemática Iberoamericana, **19** (2003), 1–48.
[22] J. A. Carrillo and G. Toscani. *Asymptotic L^1-decay of solutions of the porous medium equation to self-similarity.* Indiana Univ. Math. J., **49(1)** (2000), 113–142.
[23] E. De Giorgi. *New problems on minimizing movements.* Lions, Jacques-Louis (ed.) et al., Boundary value problems for partial differential equations and applications. Dedicated to Enrico Magenes on the occasion of his 70th birthday. Paris: Masson. Res. Notes Appl. Math. **29** (1993), 81–98.
[24] E. DiBenedetto and D. Hoff. *An interface tracking algorithm for the porous medium equation.* Trans. Amer. Math. Soc., **284(2)** (1984), 463–500.
[25] J. Dolbeault and B. Perthame. *Optimal critical mass in the two-dimensional Keller-Segel model in $\mathbb{R}^2$.* C. R. Math. Acad. Sci. Paris, **339(9)** (2004), 611–616.
[26] J. Dolbeaut and C. Schmeiser. *The two-dimensional Keller-Segel model after blow-up.* DCDS-A, **25** (2009), 109–121.
[27] F. Filbet. *A finite volume scheme for the Patlak-Keller-Segel chemotaxis model.* Numer. Math., **104(4)** (2006), 457–488.
[28] M. E. Gurtin and R. C. MacCamy. *On the diffusion of biological populations.* Math. Biosci., **33** (1977), 35–49.
[29] J. Haškovec and C. Schmeiser. *Stochastic particle approximation for measure values solutions of the 2D Patlak-Keller-Segel system.* Journal of Statistical Physics, **135(1)** (2009), 133–151.
[30] M. A. Herrero and J. J. L. Velazquez. *Singularity patterns in a chemotaxis model.* Mathematische Annalen, **306** (1996), 583–623.
[31] D. Horstmann. *From 1970 until present: the Keller-Segel model in chemotaxis and its consequences. II.* Jahresber. Deutsch. Math.-Verein., **106(2)** (2004), 51–69.
[32] W. Jäger and J. Kačur. *Solution of porous medium type systems by linear approximation schemes.* Numer. Math., **60(3)** (1991), 407–427.
[33] W. Jäger and S. Luckhaus. *On explosions of solutions to a system of partial differential equations modeling chemotaxis.* Trans. Amer. Math. Soc., **329(2)** (1992), 819–824.
[34] R. Jordan, D. Kinderlehrer, and F. Otto. *The variational formulation of the Fokker-Planck equation.* SIAM J. Math. Anal., **29(1)** (1998), 1–17.
[35] L. D. Landau and E. M. Lifshitz. *Fluid Mechanics.* Translated from the Russian by J. B. Sykes and W. H. Reid. Course of Theoretical Physics, Vol. 6. Pergamon Press, London, 1959.

[36] R. C. MacCamy. *A population model with nonlinear diffusion.* J. Differ. Equations, **39** (1981), 52–72.
[37] A. Marrocco. *Numerical simulation of chemotactic bacteria aggregation via mixed finite elements.* M2AN Math. Model. Numer. Anal., **37(4)** (2003), 617–630.
[38] K. Mikula. *Numerical solution of nonlinear diffusion with finite extinction phenomenon.* Acta Math. Univ. Comenian. (N.S.), **64(2)** (1995), 173–184.
[39] D. Morale, V. Capasso, and K. Oelschlaeger. *An interacting particle system modelling aggregation behavior: from individuals to populations.* J. Math. Biol., **50(1)** (2005), 49–66.
[40] F. Otto. *The geometry of dissipative evolution equations: the porous medium equation.* Commun. Partial Differential Equations, **26(1-2)** (2001), 101–174.
[41] R. E. Pattle. *Diffusion from an instantaneous point source with a concentration-dependent coefficient.* Quart. J. Mech. Appl. Math., **12** (1959), 407–409.
[42] J. Schöberl. *Netgen-an advancing front 2d/3d-mesh generator based on abstract rules.* Comput. Visal. Sci., **1** (1997), 41–52.
[43] K. Tomoeda and M. Mimura. *Numerical approximations to interface curves for a porous media equation.* Hiroshima Math. J., **13(2)** (1983), 273–294.
[44] J. L. Vázquez. *Smoothing and Decay Estimates for Nonlinear Diffusion Equations*, volume 33 of Oxford Lecture Series in Mathematics and its Applications. Oxford University Press, Oxford, 2006.
[45] J. L. Vázquez. *The Porous Medium Equation.* Oxford Mathematical Monographs. The Clarendon Press Oxford University Press, Oxford, 2007.
[46] C. Villani. *Topics in Optimal Transportation*, volume 58 of *Graduate Studies in Mathematics.* American Mathematical Society, Providence, RI, 2003.
[47] M. Westdickenberg and J. Wilkening. *Variational particle schemes for the porous medium equation and for the system of isentropic Euler equations*, submitted. (2008).

Martin Burger
Institut für Numerische und Angewandte Mathematik
Westfälische Wilhelms-Universität (WWU) Münster
Einsteinstr. 62, D-48149 Münster, Germany
E-mail address: martin.burger@wwu.de

José A. Carrillo
ICREA (Institutió Catalana de Recerca i Estudis Avançats)
and Departament de Mathemátiques
Universitat Autonóma de Barcelona
E-08193 Bellaterra, Spain
E-mail address: carrillo@mat.uab.es

Marie-Therese Wolfram
DAMTP (Department of Applied Mathematics and Theoretical Physics)
University of Cambridge, Wilberforce Road, Cambridge CB3 0WA, UK
E-mail address: M.Wolfram@damtp.cam.ac.uk